ACS OMEGA

http://pubs.acs.org/journal/acsodf

Article

Research on Key Technologies to Improve Cementing Displacement Efficiency

Jingpeng Wang, Youming Xiong,* Zongyu Lu, Wei Zhang, Jiwei Wu, Ruihua Wei, and Xiaoxiao Li

Cite This: *ACS Omega* 2022, 7, 37039−37049

Read Online

ACCESS | Metrics & More | Article Recommendations

ABSTRACT: The annulus has a wide and narrow clearance due to casing eccentricity in the cementing process and due to the eccentricity of casing in the process of cementing. Because the flow resistance of the drilling fluid in the wide gap is less than that in the narrow gap, the phenomena of a delayed flow or even an overall nonflow occurs in the narrow gap. Based on the existing displacement efficiency calculation model, this paper establishes the cementing displacement efficiency model under the condition of oil-based drilling fluid, explores the residual layer thickness of drilling fluid on the casing side and the sidewall side, and then links the annular displacement efficiency to the injection displacement in combination with the circulating mode resistance pressure drop formula so as to explore the change in the cementing displacement efficiency under different displacements. Considering the change in the physical parameters of annulus fluid, the change in annulus displacement efficiency is obtained. On this basis, the relationship between the wellhead cement injection flow and the annulus retention layer is studied; then, the displacement is calculated. The reasonable cementing displacement is calculated by combining the displacement with annulus displacement efficiency. The results show that the thickness of the annular detention layer increases with the increase in the casing eccentricity in the same well depth, and the growth rate of the detention layer on the wellbore side is greater than that on the casing side at the same circumferential angle. The greater the displacement, the greater the annular circulation pressure drop and circulation equivalent density, thus increasing the cementing risk. The displacement is reasonably designed. The research results in this paper have a certain guiding significance for improving the displacement rate of isolation fluid under oil-based drilling fluid conditions.

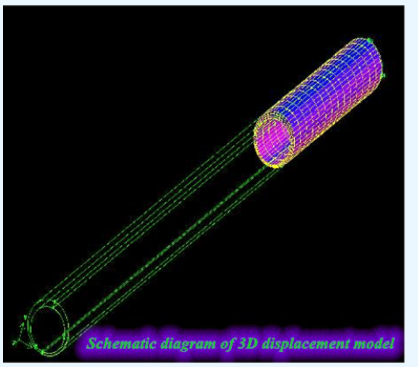

1. INTRODUCTION

Oil-based drilling fluid has many advantages, such as stable performance, strong antipolluting ability, and strong inhibition, and is widely used in China. The cementing quality under this condition is greatly affected by the effectiveness of the isolation fluid.[1−4] Cementing displacement has always been a difficulty and key point in cementing research.[5−7] For more than half a century, scholars around the world have performed systematic and in-depth studies on the mechanism and process of cement injection displacement.[8]

The specific research contents can be summarized from the point of view of three aspects: theoretical analysis of displacement mechanism, experimental research, and numerical simulation. Mahmoud[9] and others put forward the critical dynamic shear force through theoretical research and pointed out that reducing the static shear force of drilling fluid and increasing the slurry density difference could improve the cement slurry displacement effect. Parker[10] and others observed that the drilling fluid retained at the hole diameter enlargement can be effectively replaced by a low-speed plug flow. Haut et al.[11−13] concluded that the displacement effect of cement slurry was affected by mud cake state and drilling fluid. In addition, they also put forward the concept of the nonflow coefficient of the drilling fluid. Zhang et al.[14] summarized the latest achievements of cement injection displacement technology in the West at that time.

The mechanism and technology of cement injection displacement, the influence of cement slurry performance, and the rheology of the displacement effect were also introduced in detail elsewhere. Many scholars have also made a systematic study of the flow law of eccentric annulus.[15] Heyda[16] studied the axial velocity field of the Newtonian fluid in eccentric annuli by using Green's function method. Redberge[17] used the above method to solve the dimensionless flow distribution of the axial stable laminar flow of Newtonian fluid. Vaugh et al.[18] treated the eccentric annulus into a variable height channel and studied the axial steady laminar flow distribution of the power-law fluid. Iyoho and Azar[19] improved the calculation method of the

Received: January 20, 2022
Accepted: May 18, 2022
Published: October 12, 2022

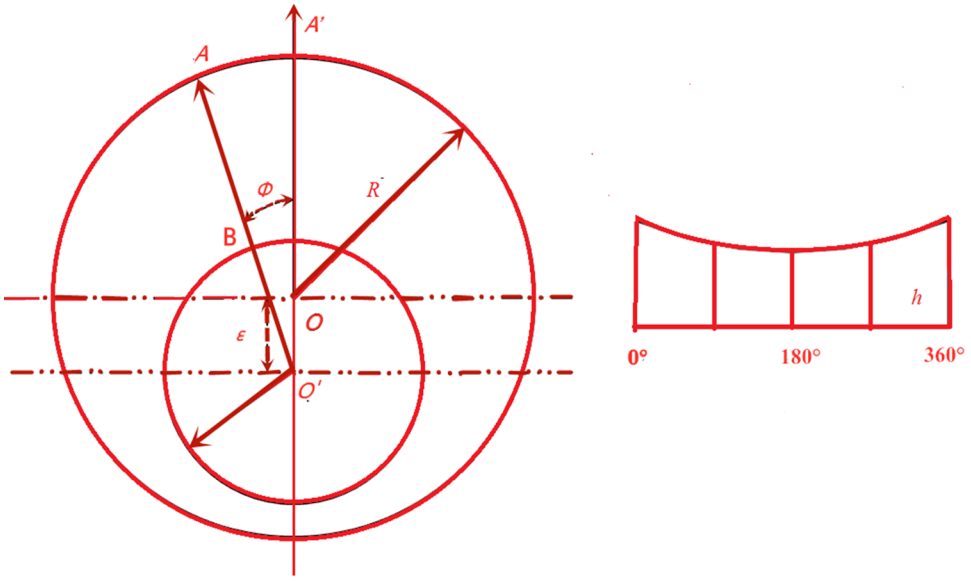

Figure 1. Eccentric annulus diagram.

groove height. Tosun[20] applied Iyoho's method to the flow calculation of Newtonian and non-Newtonian fluids. Robertson[21] analyzed the axial flow law of the Bingham fluid in the narrow gap of an eccentric annulus. Beirut[22] studied the flow characteristics of the elastic−plastic fluid in eccentric annuli. Cloud[23] and others used a two-dimensional model to deduce the velocity variation and particle migration law of slurry in an eccentric annulus in wide and narrow gaps.

In the cementing process, due to casing eccentricity, wide and narrow gaps are generated in the annulus. Since the flow resistance received by the drilling fluid in the wide gap is less than that in the narrow gap, the retention phenomenon of a delayed flow or even an overall no flow occurs in the narrow gap.[24−26] Both the isolation fluid and the drilling fluid are non-Newtonian fluids. They do not flow as a whole but flow in layers along the annulus direction. The shear stress between the flow layers of the same fluid is a kind of resistance.

This resistance is related to the viscosity density and other properties of the fluid. The higher the flow rate, the smaller the interlayer shear stress. The lowest interlayer resistance corresponds to the position with the maximum velocity.[27−29] When two fluids with different properties are replaced, the shear stress of the displaced fluid is the driving force that causes the fluid to flow. At the interface of the fluid contact, the closer the fluid is to the outer layer, the greater the shear stress.[30−32]

In this paper, the efficiency of the spacer fluid to replace the drilling fluid is analyzed. It is necessary to analyze the displacement boundary. The displacement efficiency can be calculated according to the thickness of the retained layer at the annulus boundary and the penetration degree of the displacement fluid. According to the displacement interface model, reasonable measures to improve the displacement efficiency and reduce the retention of drilling fluid can also be calculated. Therefore, it is of great significance to analyze the retention of drilling fluid for studying the efficiency of the cement slurry to displace the drilling fluid.

2. REPLACE THE MATHEMATICAL MODEL

2.1. Casing Eccentricity Calculation Model. As shown in Figure 1, if the casing of $d(2r)$ is run into the hole with a diameter $D(2R)$, its eccentricity $\overline{OO} = \varepsilon$. Due to casing eccentricity, the gap $h = \overline{AB}$ at different positions changes.

The casing eccentricity can be expressed by eccentricity e

$$e = \varepsilon/(R - r) \tag{1}$$

The clearance y of each position in eccentric annulus space can be expressed as follows

$$y = \overline{O'A} - \overline{O'B} = \varepsilon \cos\phi + \sqrt{R^2 - \varepsilon^2 \sin^2\phi} - r \tag{2}$$

Therefore, in the above formula, ϕ scope is 0 and π. The width of the widest and the narrowest gap in the eccentric annulus can be obtained as follows

$$y_w = R - r - \varepsilon = (R - r)(1 + e) \tag{3}$$

$$y_n = R - r - \varepsilon = (R - r)(1 - e) \tag{4}$$

2.2. Boundary Calculation Model of the Displacement Detention Layer. To analyze the efficiency of the spacer fluid to replace the drilling fluid, it is necessary to analyze the displacement boundary. The displacement efficiency can be calculated according to the thickness of the retained layer at the annular boundary and the penetration degree of the displacement fluid. According to the displacement interface model, reasonable measures to improve the displacement efficiency and reduce the retention of drilling fluid can also be calculated.

Replacing the drilling fluid with the spacer fluid is a very complex process because both of them are non-Newtonian fluids. Very complex physical and chemical phenomena occur at the displacement interface.[33,34] To simplify the study, the following assumptions are made:

(1) The isolation fluid is in direct contact with the drilling fluid.

(2) Both the drilling fluid and the spacer fluid are Bingham fluids, and there is no wall slip in the process of displacement.

(3) The influence of mixing, diffusion at the interface, and chemical action after the contact of the isolation fluid and the drilling fluid on displacement flow are ignored.

https://doi.org/10.1021/acsomega.2c00419
ACS Omega 2022, 7, 37039−37049

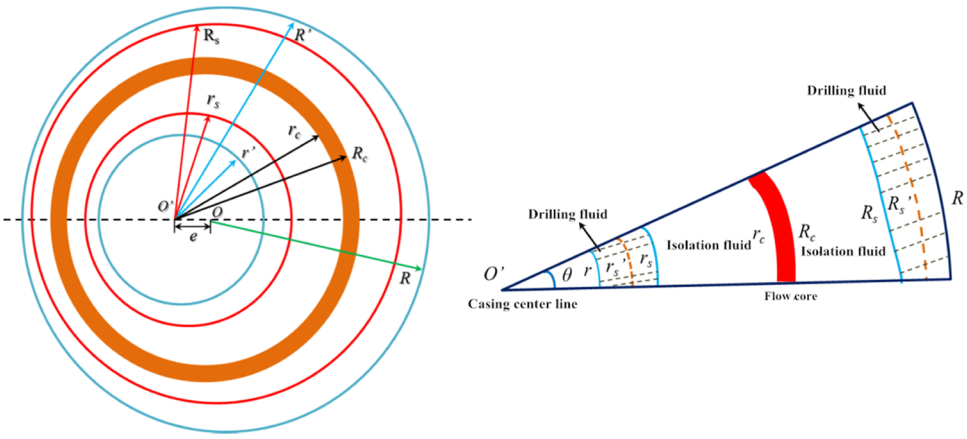

Figure 2. Profile of the annular spacer displacement.

(4) The effect of mud cake on the performance of drilling fluid at the sidewall is not considered (the properties of drilling fluid are rheology, water loss, plastic viscosity, dynamic shear force, etc).

Figure 2 is the profile map of the annular spacer fluid displacement at a certain time, where r is the inner diameter of the annulus, R is the outer diameter of the annulus, r_c is the inner diameter of the flow core, R_c is the outer diameter of the flow core, r_s and R_s are the interfaces between the spacer fluid and the drilling fluid at a certain time, r_s' and R_s' are any positions in the drilling fluid layer near the casing side and near the wellbore once, respectively, and θ is the profile angle.

If the distance from any point in the annulus to the center of the borehole is r, then the equation of fluid flow in the annulus can be obtained according to fluid mechanics

$$\rho\left(\frac{\partial uz}{\partial t} + ur\frac{\partial uz}{\partial r} + \frac{u\varphi}{r}\frac{\partial uz}{\partial \varphi} + uz\frac{\partial uz}{\partial z}\right) = -\frac{\partial P}{\partial z} + \left[\frac{1}{r}\frac{\partial}{\partial r}(r\tau rz) + \frac{1}{r}\frac{\partial u\varphi z}{\partial \varphi} + \frac{\partial \tau rz}{\partial z}\right] \quad (5)$$

where u_r is the radial velocity, m/s; u_z is the axial velocity, m/s; u_φ is the circumferential velocity, m/s; ρ is the fluid density, g/cm^2; τ_{rz} is the longitudinal dynamic shear force, Pa; $u_{\varphi z}$ is the circumferential dynamic shear force, Pa; and g is the acceleration of gravity, m/s^2.

Due to the axial fluid displacement, there are

$$u_r = 0, \quad u_\varphi = 0 \quad (6)$$

Because it is a stable system and uniform flow

$$\frac{\partial uz}{\partial t} = 0, \quad \frac{\partial uz}{\partial z} = 0, \quad \frac{\partial \tau rz}{\partial z} = 0 \quad (7)$$

$\frac{1}{r}\frac{\partial}{\partial r}(r\tau rz)$ is a very small quantity relative to other quantities and can be regarded as 0. Therefore, formula (5) can be rewritten as follows

$$\frac{\partial t}{\partial r} + \frac{\tau}{r} = \frac{\partial P}{\partial z} \quad (8)$$

The partial differential equation shown in eq 8 is transformed into an ordinary differential equation and solved

$$\tau = -\frac{1}{2}r\frac{\Delta P}{\Delta L} + \frac{c}{r} \quad (9)$$

where c is an arbitrary constant.

According to the rheological properties of the Bingham fluid, it can be seen that at the boundary of the flow core

$$\tau|_{r=r_c=R_c} = \tau_{HBc} \quad (10)$$

where τ_{HBc} is the Heba fluid shear stress.

It can be seen from the above equation that the shear stress distribution of the Bingham fluid in the annulus is as follows

$$\tau = \left[\frac{1}{2}r_c\frac{\Delta P}{\Delta L} + \tau_{HBc}\right]\frac{r_c}{r} - \frac{1}{2}r\frac{\Delta P}{\Delta L}r \le r_c \quad (11)$$

$$\tau = \left[\tau_{HBc} - \frac{1}{2}R_c\frac{\Delta P}{\Delta L} + \right]\frac{R_c}{r} + \frac{1}{2}r\frac{\Delta P}{\Delta L}r \ge R_0 \quad (12)$$

The relationship between the width of flow core, pressure drop, and dynamic shear force is as follows

$$\frac{\Delta P}{\Delta L}(R_c - r_c) = 2\tau_0 \quad (13)$$

The cementing process is a process in which the isolation fluid replaces the drilling fluid and occupies the annulus. The displacement starts from the most prominent flow core, that is, the position with the maximum flow velocity. With the process of jacking, the displacement interface begins to expand until the displacement power and the yield stress of the drilling fluid reach a mechanical balance, that is, the driving force of the isolation fluid at this position is not enough to overcome the yield of the drilling fluid itself. The stress causes the fluid to flow. At this moment, the displacement interface forms a stable displacement boundary, and the annulus is filled with the isolating fluid to the maximum extent. At this time, the replacement efficiency is the highest. The replacement process is shown in Figure 3.

The microelement of the drilling fluid with an angle of $\Delta\theta$ when the displacement interface near the casing side is not stable is taken as the analysis object. Although the drilling fluid has not yet been replaced by the isolation fluid, it is affected by the displacement pressure, interfacial shear stress, buoyancy caused by the density difference between the two fluids, and its own bending stress.

The microelement of drilling fluid layer with a height of dl is between r_s and r_s'. The mechanical model is shown in Figure 3. The displacement pressure is F_1, the buoyancy caused by density difference is F_2, the shear stress caused by the isolation fluid flow is the displacement force F_3, and the yield stress of the drilling fluid itself is the flow resistance F_4.

https://doi.org/10.1021/acsomega.2c00419
ACS Omega 2022, 7, 37039−37049

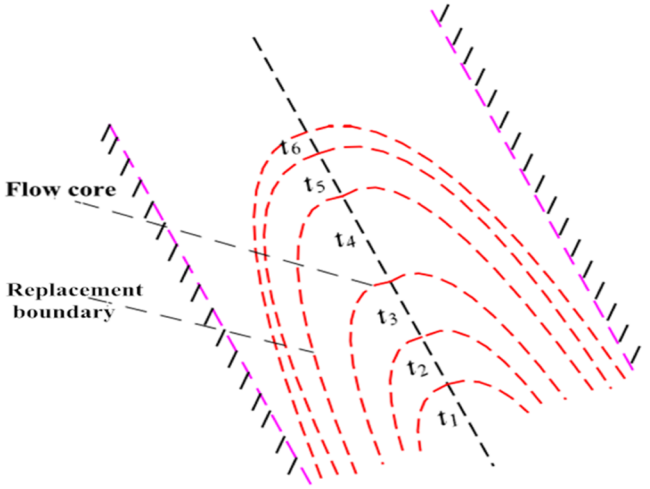

Figure 3. Displacement interface changes with time.

Using an oil-based drilling fluid, new requirements for cementing technology are put forward. Oil-based drilling fluid is different from the general water-based drilling fluid. In the formation, because the oil-based drilling fluid contacts with the formation for a long time, the wettability of the formation is reversed, and some or more rock surfaces are lipophilic. The replacement of the drilling fluid with the spacer fluid is affected not only by gravity and friction but also by the interfacial tension because the wetting contact angle is less than 90°.

For an oil-based drilling fluid, there is an additional adhesion during the displacement process, and its expression is shown in Figure 4.

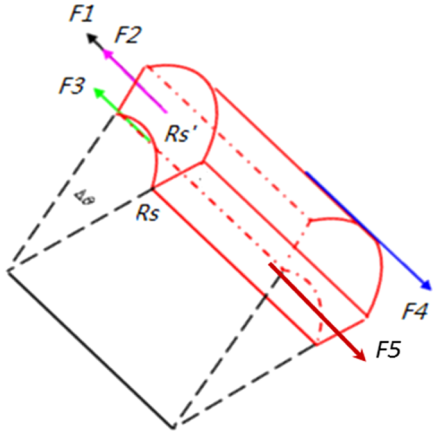

Figure 4. Force diagram of an oil-based drilling fluid.

In this case, S is the cross-sectional area of microelements, m^2; τ_0 is the shear stress of the drilling fluid at r_s, Pa; S_1 is the inner wall surface area of the microelement, m^2; S_2 is the surface area of the outer wall, m^2; $\Delta P/\Delta L$ is the driving pressure gradient; ρ_m is the density of the drilling fluid, g/cm^3; and ρ_g is the density of the isolation fluid, g/cm^3.

According to the shear stress distribution of the fluid flowing in the annulus, the displacement pressure F_1 produced by the isolation fluid flow on the displacement interface of the drilling fluid in contact with it is

$$F_1 = \frac{\Delta P}{\Delta L} S = \frac{1}{2}\frac{\Delta P}{\Delta L}(r_s'^2 - r_s^2)\, \mathrm{d}\theta \mathrm{d}l \tag{14}$$

The buoyancy force F_2 produced by density difference is

$$F_2 = \frac{1}{2}\Delta\rho(r_s'^2 - r_s^2)\, g\mathrm{d}\theta \mathrm{d}l \tag{15}$$

The wall shear force F_3 produced by the flow of spacer fluid on drilling fluid is

$$F_3 = \tau_0 S_1 = \tau_2 r_s \mathrm{d}\theta \mathrm{d}l = \left[\left[\frac{1}{2} r_c \frac{\Delta P}{\Delta L} + \tau_{HBc}\right] r_c - \frac{1}{2} r_s^2 \frac{\Delta P}{\Delta L}\right] \mathrm{d}\theta \mathrm{d}l \tag{16}$$

The wall shear stress F_4 hindering the flow in the drilling fluid is

$$F_4 = \tau_1 r_s' \mathrm{d}\theta \mathrm{d}l \tag{17}$$

When the oil-based drilling fluid is in contact with the wellbore rock for a long time, the wettability of the rock on the wellbore surface may be reversed. Then, the contact angle between the oil-based drilling fluid and the rock is less than 90°, which shows that it is lipophilic or strongly lipophilic. In the cementing process of the conventional drilling fluid, the influence of the adhesion caused by wettability in the process of displacement is very small because the wettability of the conventional drilling fluid is consistent with that of the spacer fluid; compared with the slight effect of adhesion on the displacement of conventional drilling fluid, the wettability reversal of the rock shows lipophilicity, which has a greater impact on the displacement of the oil-based drilling fluid.

When $\theta < 90°$, the rocks are lipophilic.[33,34] In the process of displacement, the drilling fluid near the wellbore suffers an additional resistance, adhesion F, which is named F_5 in this paper.

$$F_5 = \gamma \cos\beta \tag{18}$$

where γ is the interfacial tension, mN/m, and β is the wetting contact angle,°.

According to the mechanical equilibrium, $F_1+F_2+F_3 = F_4+F_5$. It can be concluded that the shear stress in r_s is

$$\tau_1 = \left[(r_s'^2 - r_s^2)\left(\frac{\Delta P}{\Delta L} - \rho_m g + \rho_g g\right) + \frac{\Delta P}{\Delta L}(R_c r_c - r_s^2) - 2 \times 10^{-3} r\gamma \cos\beta\right] / (2r_s') \tag{19}$$

It can be seen from eq 19 that the shear stress τ_1 of the drilling fluid close to the casing wall is related to the boundary position r_s and the microelement location r_s'.

The retention mechanism of the drilling fluid can be obtained here because both the displacing fluid and the displaced fluid are non-Newtonian fluids and stratified flow occurs during the flow, resulting in the fluid flow at the displacement boundary. As the displacement interface expands toward the boundary, the shear stress on the drilling fluid at the boundary decreases. When the shear stress is less than the yield stress of the drilling fluid, the displacement interface stops expanding. This results in the formation of a stable displacement boundary. This in turn results in no flow of the drilling fluid and the formation of a drilling fluid retention layer at the wellbore.

2.3. Research on the Calculation Model for Displacement Boundary Position. *2.3.1. Calculation Model for Boundary Position of Displacement Interface at One Side of Casing.* As can be seen from the above formula, the smaller the r_s, the larger the τ_1; that is, the drilling fluid layer out of the casing

https://doi.org/10.1021/acsomega.2c00419
ACS Omega 2022, 7, 37039−37049

bears the maximum shear stress. Therefore, the drilling fluid at the casing should flow first if the drilling fluid is to flow. However, in the actual displacement process, the drilling fluid at the casing does not flow first because the fluid always flows from the position where there is the least resistance before the force is transferred to the casing. The shear stress of the drilling fluid layer at the displacement interface r_s' is greater than its dynamic shear stress, so it is necessary to redefine r_s' and conduct a new stress analysis. Therefore, with the increase in displacement contact time, the displacement boundary gradually extends from the position of maximum velocity in the annulus to both sides, the interface between the isolation fluid and the drilling fluid gradually expands, and the shear stress of the drilling fluid at the annulus boundary gradually decreases until it is equal to the dynamic shear force of the drilling fluid τ_0, namely,

$$\tau_1 = \tau_0 \tag{20}$$

At this time, the displacement interface is stable. Because the drilling fluid cannot overcome its own viscous force, the displacement interface does not expand, forming a stable displacement boundary, and the drilling fluid from the displacement boundary to the casing is truly retained. According to the equilibrium condition in which the displacement interface is stable in the process of displacing drilling fluid with the isolation fluid, the boundary of the casing out of the retained layer can be obtained as follows

$$r_s = \sqrt{\frac{2r\tau_0 + 2\times 10^{-3} r\gamma\cos\beta - \frac{\Delta P}{\Delta L}(R_c r_c - r^2)}{\rho_g g - \rho_m g} + r^2} \tag{21}$$

The thickness of the retained layer at the casing is

$$h = r_s - r = \sqrt{\frac{2r\tau_0 + 2\times 10^{-3} r\gamma\cos\beta - \frac{\Delta P}{\Delta L}(R_c r_c - r^2)}{\rho_g g - \rho_m g} + r^2} - r \tag{22}$$

2.3.2. Calculation Model for Boundary Position of Displacement Interface on One Side of Wellbore. According to the analysis results of the casing wall, the mechanical equilibrium equation of the wellbore is as follows.

The displacement pressure F_1 of microelements is

$$F_2 = \frac{\Delta P}{\Delta L} S = \frac{1}{2}\frac{\Delta P}{\Delta L}(R_s'^2 - R_s^2)\,\mathrm{d}\theta\mathrm{d}l \tag{23}$$

The buoyancy force F_2 produced by density difference is

$$F_2 = \frac{1}{2}\Delta\rho\,(R_s'^2 - R_s^2)\,g\,\mathrm{d}\theta\mathrm{d}l \tag{24}$$

The wall shear force F_3 produced by the flow of spacer fluid on drilling fluid is

$$F_3 = \tau_0 S_1 = \tau_2 R_s \mathrm{d}\theta\mathrm{d}l = \left[\left[\tau_2 - \frac{1}{2}R_c\frac{\Delta P}{\Delta L}\right]R_c + \frac{1}{2}R_s^2\frac{\Delta P}{\Delta L}\right]\mathrm{d}\theta\mathrm{d}l \tag{25}$$

The wall shear stress F_4 hindering the flow in the drilling fluid is

$$F_4 = \tau_1 R_s'\,\mathrm{d}\theta\mathrm{d}l \tag{26}$$

The adhesion force of drilling fluid F_5 near the wellbore is

$$F_5 = \gamma\cos\beta \tag{27}$$

According to the mechanical equilibrium, $F_1+F_2+F_3 = F_4+F_5$. The boundary of R_S is obtained as follows

$$R_s = \sqrt{\frac{\frac{\Delta P}{\Delta L}(R^2 - R_c r_c) - 2R\tau_0 - 2\times 10^{-3} R\gamma\cos\beta}{\rho_g g - \rho_m g} + R^2} \tag{28}$$

The thickness of the retained layer at the wellbore is

$$H = R - R_s = R - \sqrt{\frac{\frac{\Delta P}{\Delta L}(R^2 - R_c r_c) - 2R\tau_0 - 2\times 10^{-3} R\gamma\cos\beta}{\rho_g g - \rho_m g} + R^2} \tag{29}$$

2.4. Displacement Efficiency Calculation of the Oil-Based Drilling Fluid. According to the borehole geometry, the displacement efficiency of the profile and the overall displacement efficiency of the annulus interface under different circumferential angles can be deduced. In other words, the displacement efficiency of the profile η_θ at any circumferential angle is

$$\eta_\theta = \frac{\pi(R_s^2 - r_s^2)}{\pi(R^2 - r^2)} \tag{30}$$

The displacement efficiency on the cross-sectional area of the whole annulus is

$$\eta = \frac{\int_0^{2\pi}(R_s^2 - r_s^2)\,\mathrm{d}\theta}{\int_0^{2\pi}\pi(R^2 - r^2)\,\mathrm{d}\theta} \tag{31}$$

The annular friction pressure drop formula of the Bingham fluid can be expressed as follows

$$\frac{\Delta P}{\Delta L} = \frac{24\eta_s Q - 8\pi\tau_0\left[2\left(\frac{R^2 - r^2}{2\ln\frac{R}{r}}\right)^{3/2} - (R^3 + r^3)\right]}{3\pi\left[R^4 - r^4 - \frac{(R^2 - r^2)^2}{\ln\frac{R}{r}}\right]} \tag{32}$$

It can be seen from the above formula that

$$\eta = \frac{\int_0^{2\pi}\left[\frac{\frac{\Delta P}{\Delta L}(R^2 - r^2) - 2R\tau_0 - 2r\tau_0}{\rho_g g - \rho_m g} + R^2 - r^2\right]\mathrm{d}\theta}{\int_0^{2\pi}(R^2 - r^2)\,\mathrm{d}\theta} \tag{33}$$

Through the above two formulas, the relationship between the amount of spacer and the displacement efficiency can be established.

This section analyzes the influence of casing eccentricity on jacking efficiency, establishes the model, and analyzes that the displacement boundary is essential. The displacement efficiency in the cementing process can be calculated according to the thickness of the retention layer at the annulus boundary and the penetration degree of the displacement fluid. The reasonable measures to improve the displacement efficiency and reduce the retained drilling fluid can also be calculated according to the displacement interface model.

https://doi.org/10.1021/acsomega.2c00419
ACS Omega 2022, 7, 37039−37049

Table 1. Basic Parameters of Simulation

parameter name	numerical unit	parameter name	numerical unit
well depth	5000 m	drilling fluid density	2.2 g/cm^3
construction displacement	0.033 m^3/min	plastic viscosity of drilling fluid	0.053 Pa.s
density of isolation fluid	2.42 g/cm^3	dynamic shear force of drilling fluid	9.47 Pa
injection temperature	20 °C	construction time	120 min
plastic viscosity of isolation fluid	0.053 Pa.s	isolation hydraulic shear force	13.4 Pa
casing radius	244.5 mm	well diameter	311.12 mm

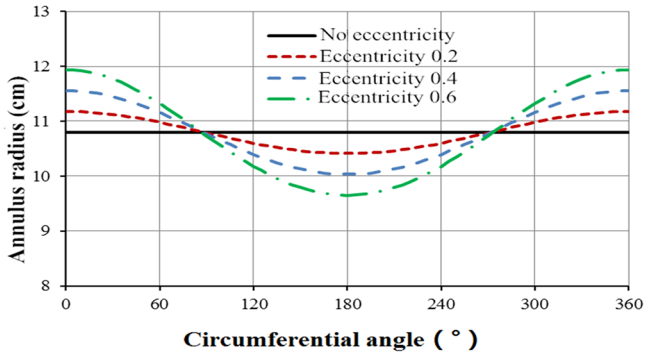

(a) Relationship between annulus radius and well circumferential angle

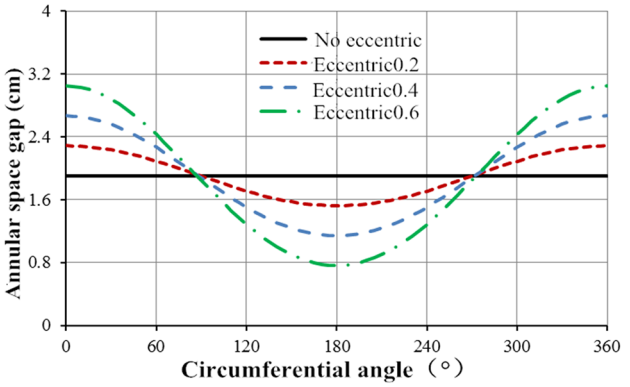

(b) Relationship between annular space gap and well circumferential angle

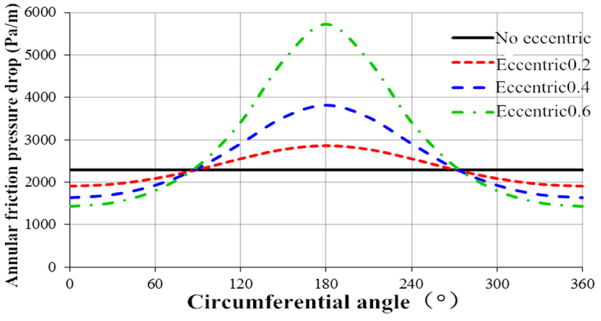

(c) Relationship between annular friction pressure drop and wellbore circumferential angle

Figure 5. Relationship between annular radius, annular space gap, annular friction, and wellbore circumferential angle.

3. RESULTS AND DISCUSSION

In this paper, the calculation data are from a well in the field. According to the field cementing operation process, the influence of displacement efficiency of the spacer fluid under oil-based drilling fluid conditions is analyzed. Table 1 shows the field basic parameters used for simulation calculation.

3.1. Relationship between Casing Eccentricity and Borehole Circumferential Angle. After studying the relationship among the annulus radius, annular space gap, and borehole circumferential angle under the condition of different casing eccentricities from Figure 5a,b, it can be seen that the annulus radius and the annular space gap at 0 and 2 π gradually increase with the increase in casing eccentricity, while the annulus radius and annular space gap at π gradually decrease. Therefore, the ratio of the annular space gap width becomes larger and larger with the increase in eccentricity, which affects the fluid velocity and pressure drop distribution in the narrow and wide areas and affects the displacement efficiency.

It can be seen from Figure 5c that when the casing is not eccentric, the circulating friction pressure drop in the annular section of the well is uniformly distributed along the circumferential angle of the well. As the eccentricity increases, the friction pressure drop at 0 and 2π decreases due to the larger annular space gap at 0 and 2 π and the friction pressure drop at π increases due to the small annular space gap at π. Therefore, the annular space clearance is the main factor affecting the annular friction pressure drop.

3.2. Effect of Drilling Fluid Retention Zone. In the process of cementing, the annular space is wide and narrow because of casing eccentricity. The phenomenon of delayed flow or even overall nonflow occurs in the narrow gap because the flow resistance received by drilling fluid at the wide gap is less than that at the narrow gap.

It can be seen from Figure 6 that under the condition of isolating fluid displacement of 23 L/s, the thickness of the retention layer at the casing side and well wall side also increases with the corresponding increase in casing eccentricity. The thickness of the retention layer at the borehole side is greater than that at the casing side. In addition, under different eccentricity conditions, the thickness of the retained layer is the thinnest when the hole circumferential angle is 0 and 2 π, and the maximum thickness is found when the circumferential angle is π. According to the pressure distribution diagram of the annulus interface, the pressure is the highest when the circumferential

https://doi.org/10.1021/acsomega.2c00419
ACS Omega 2022, 7, 37039−37049

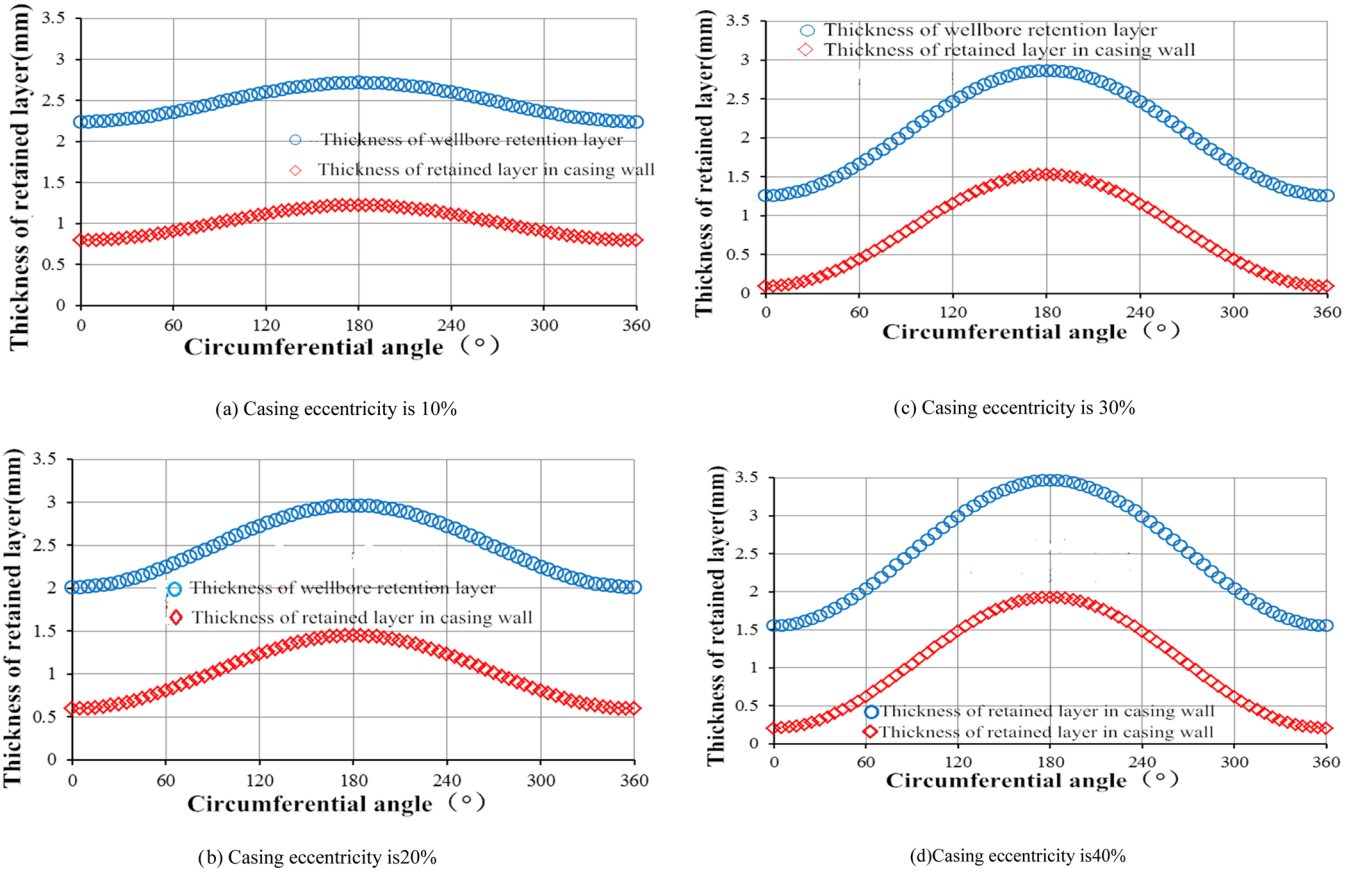

Figure 6. Thickness of the drilling fluid retained in the wellbore and casing under different casing eccentricity conditions with the displacement of 23 L/s.

angle is 0 or 2 π and it is the lowest when the circumferential angle in π. The high-pressure point causes the annular fluid to pass through the section better. Therefore, the thickness of the retained layer on the wellbore and casing side is inversely proportional to the annular pressure.

Figure 7 shows the relationship between the thickness of the remaining layer with different casing eccentricity delays under the condition of isolation fluid displacement of 33 L/s. From the figure, it can be seen that there is no retained drilling fluid on the casing wall in the 0 and 2 π directions, while there is a part of retained drilling fluid in the π direction. With the increase in casing eccentricity, the thickness of the retained drilling fluid continues to increase when the circumferential angle is π. Compared with the retention thickness under the condition of displacement of 23 L/s, the thickness of the retention layer will be significantly lower at 33 L/s.

Figure 8 shows the relationship between the thickness of the remaining layer with different casing eccentricities and time delays under the condition of isolation fluid displacement of 43 L/s. It can be seen from the figure that when the casing eccentricity is 1%, there is almost no retained drilling fluid on the casing side; when the eccentricity is 20%, there is no retained drilling fluid in the circumferential angle direction of other wells except for the retained drilling fluid on the casing wall at 120−240°. At the same time, the drilling fluid retained on the casing side increases with the increase in casing eccentricity, and the thickness of the drilling fluid retained on the sidewall increases gradually. However, the retained thickness is less than that at 33 L/s. Therefore, under downhole conditions, displacement pressure drop also increases with the increase in drilling fluid displacement, which is helpful in improving the displacement.

3.3. Influence of Isolation Fluid Displacement. In the process of cementing operation, the annular circulation pressure drop and circulation equivalent density also increase significantly when the displacement is larger, which increases the cementing risk.

Figure 9 shows the relationship between casing eccentricity and displacement efficiency, annular circulation pressure drop, and annular equivalent circulation density under different displacements. Figure 9a shows that under the condition of the same eccentricity, the displacement efficiency improves with the increase in drilling fluid displacement; at the same time, the annular displacement efficiency gradually decreases with the increase in casing eccentricity under the same displacement. Therefore, the displacement efficiency can be improved by increasing the injection displacement. However, it can be seen from Figure 9b that the annular circulation friction pressure drop and the wellbore equivalent circulation density increase with the increase in injection rate. It can be seen from Figure 9c that the model pressure drop in the annulus increases exponentially when the displacement of the spacer fluid increases by 10 L/s. for low-pressure and easily lost circulation formations, cementing risks and downhole complications will occur. Therefore, it is necessary to design displacement under reasonable conditions.

3.4. Influence of Drilling Fluid Dynamic Shear Force. In this paper, the dynamic shear force of the isolation fluid is 13.4 Pa, while that of the drilling fluid is 9.47 Pa. By changing the dynamic shear force of the drilling fluid, the relationship

https://doi.org/10.1021/acsomega.2c00419
ACS Omega 2022, 7, 37039−37049

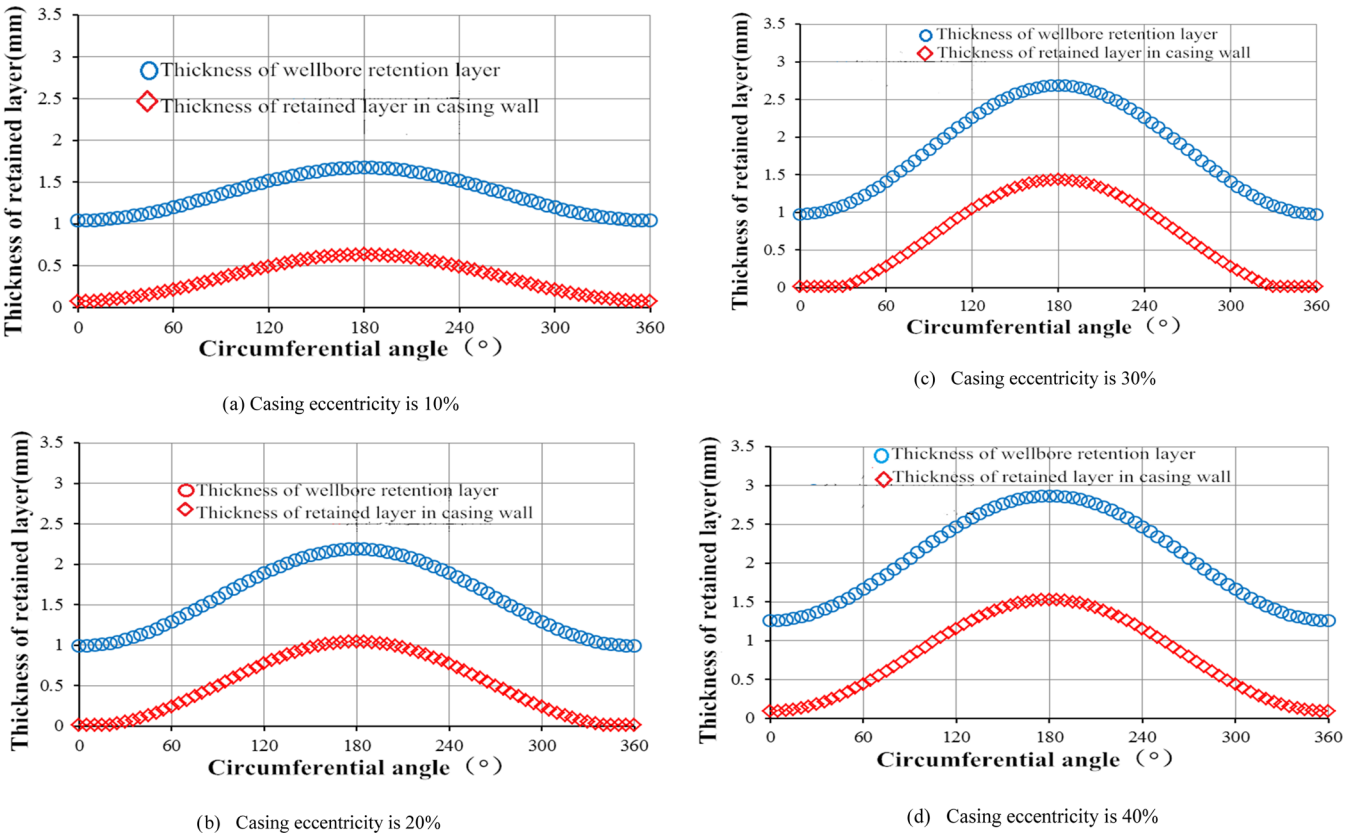

(a) Casing eccentricity is 10%

(c) Casing eccentricity is 30%

(b) Casing eccentricity is 20%

(d) Casing eccentricity is 40%

Figure 7. Thickness of the drilling fluid retained in wellbore and casing under different casing eccentricity conditions with the displacement of 33 L/s.

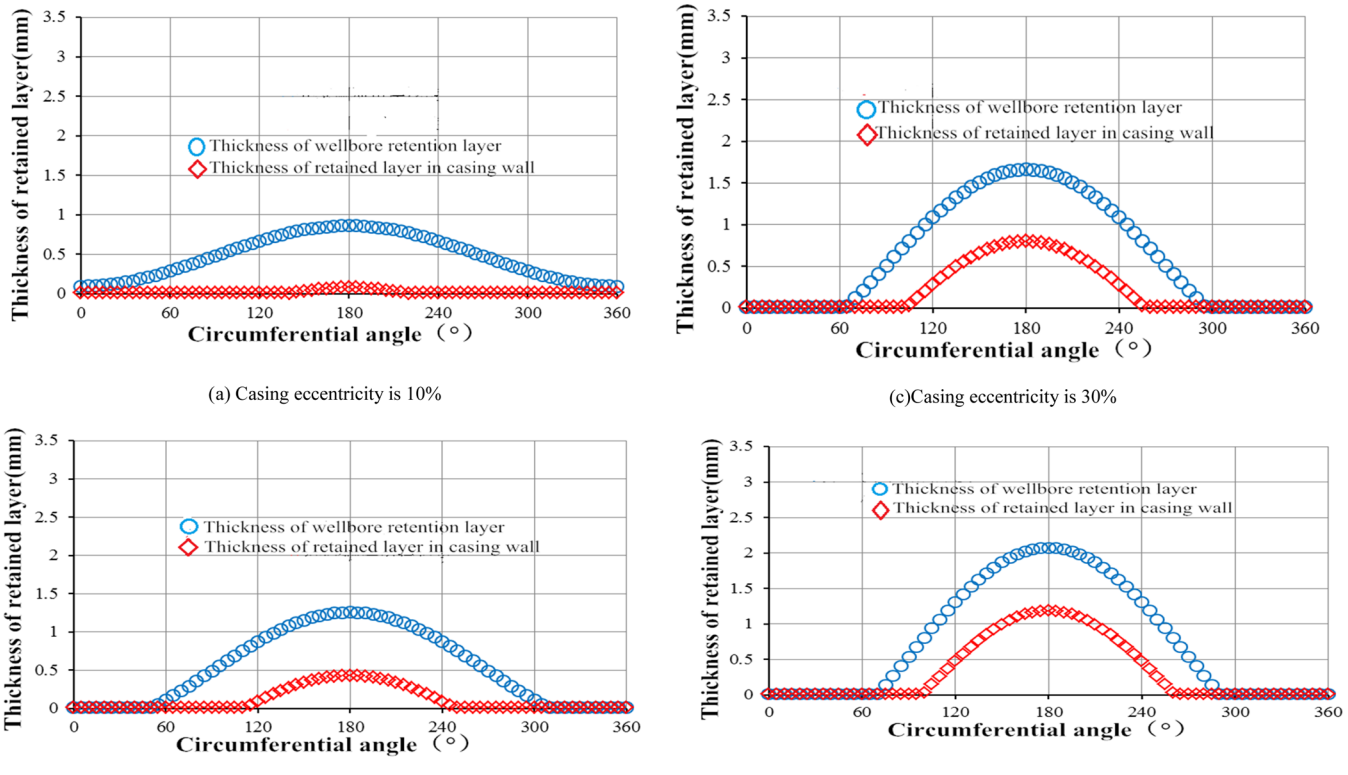

(a) Casing eccentricity is 10%

(c)Casing eccentricity is 30%

(b) Casing eccentricity is 20%

(d) Casing eccentricity is 40%

Figure 8. Thickness of the drilling fluid retained in wellbore and casing under different casing eccentricity conditions when the displacement is 43 L/s.

between the dynamic shear force of the drilling fluid and the displacement efficiency is obtained. By increasing or decreasing the dynamic shear force of drilling fluid, it can be seen that the dynamic shear force of the drilling fluid changes linearly with the

https://doi.org/10.1021/acsomega.2c00419
ACS Omega 2022, 7, 37039−37049

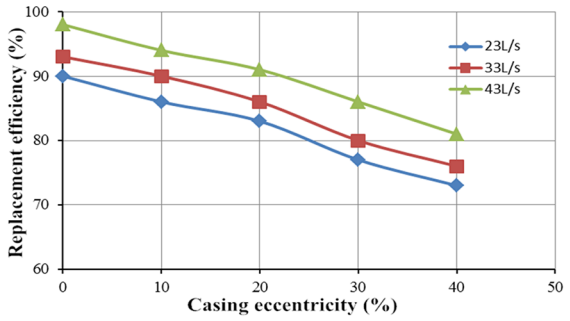

(a) Relationship between casing eccentricity and displacement efficiency under different displacement conditions

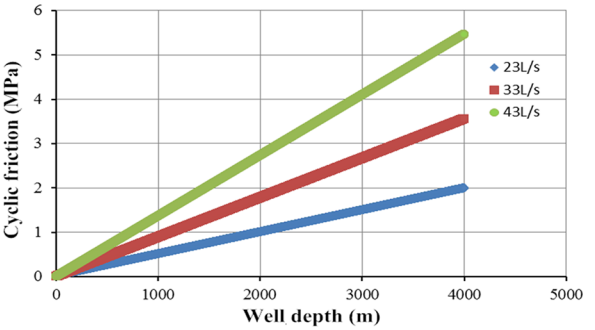

(b) Pressure drop of annular circulation with different displacement

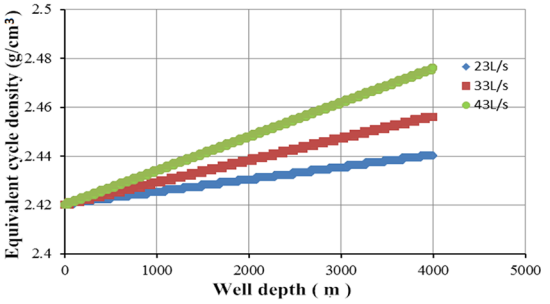

(c) Displacement of annular space under different displacement densities

Figure 9. Relationship among casing eccentricity and displacement efficiency, annular circulation pressure drop, and annulus equivalent circulation density under different displacements.

displacement efficiency. It can be seen from Figure 10 that when the casing eccentricity is 10%, the greater the dynamic shear

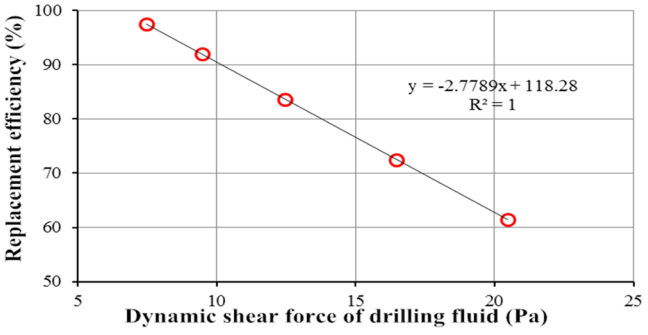

Figure 10. Relationship between drilling fluid dynamic shear force and displacement efficiency when the casing eccentricity is 10%.

force, the lower the displacement efficiency and the smaller the dynamic shear force, the higher the displacement efficiency. Therefore, displacement efficiency and cementing quality can be improved by adjusting the performance of the drilling fluid.

3.5. Influence of Isolation Fluid Density. The densities of the isolation and drilling fluids are set as 2.2 and 2.42 g/cm^3, respectively. Figure 11 shows the relationship between the density of spacer fluid and displacement efficiency when the casing eccentricity is 10%. It can be seen from the figure that the displacement efficiency increases with the increase in spacer density and decreases with the decrease in spacer density. Therefore, the displacement efficiency can reach 90% when the density difference is 0.2 g/cm^3 and decreases significantly when the density difference is lower than 0.2. Therefore, the density difference between the spacer fluid and the drilling fluid has an

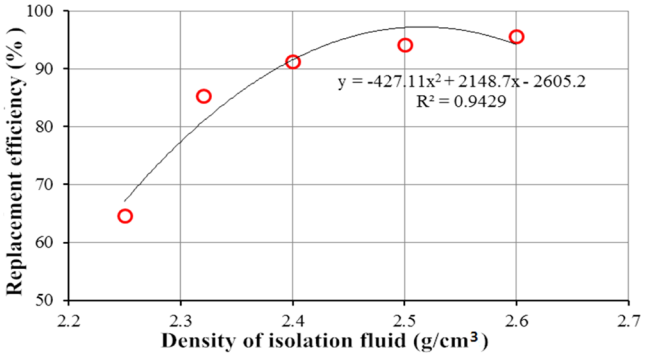

Figure 11. Relationship between the density of spacer fluid and the displacement efficiency when the casing eccentricity is 10%.

important influence on the displacement efficiency of cement injection.

4. CONCLUSIONS

On the basis of a large number of literature research and analysis, this paper explores the distribution of wellbore circulating friction and pressure drop under eccentric annulus. Based on the existing displacement efficiency calculation model, the cementing displacement efficiency model under the condition of oil-based drilling fluid is established. The thickness of the retained layer of the drilling fluid at the casing side and the well wall side is explored. Then, the annular displacement efficiency is found to be related to the injection displacement using the circulation resistance pressure drop formula. By exploring the change in the cementing displacement efficiency under different displacements and considering the change in the physical parameters of

https://doi.org/10.1021/acsomega.2c00419
ACS Omega 2022, 7, 37039−37049

annulus fluid, the change in the annular displacement efficiency is obtained. Some conclusions are drawn as follows:

1. The thickness of the annular holdup layer is obviously increased with the increase in the casing eccentricity in the same well depth. The growth rate of the retained layer on the wall side is greater than that on the casing side at the same circumferential angle. At the same well depth, the thickness of the retained layer at the casing side is smaller than that at the wall side. The thickness of the retained layer at the displacement interface decreases with the increase in the injection rate. The variation range of the casing side under the same circumferential angle is greater than that of the sidewall.
2. The thickness of the annulus retention layer has little difference between the 33 L/s isolation fluid displacement and the 43 L/s isolation fluid displacement, both of which are significantly less than the 23 L/s displacement. Therefore, the recommended on-site flushing displacement is 33 L/s.
3. Compared with the noncirculating drilling fluid, circulating drilling fluid before cementing can improve the displacement efficiency, increase the circulation time of the drilling fluid, and improve the cementing displacement efficiency. However, the improvement effect is not obvious. The annular displacement efficiency distribution is consistent with the dynamic plastic ratio of the drilling fluid.
4. The displacement efficiency reaches 95% when the density difference between the isolation fluid and the drilling fluid is 0.4 g/cm^3 but reaches 92% when the dynamic shear difference is 4 Pa.

AUTHOR INFORMATION

Corresponding Author

Youming Xiong − *State Key Laboratory of Oil and Gas Reservoir Geology and Exploitation, Southwest Petroleum University, Sichuan, Chengdu 610500, China*; Email: xiongym@swpu.edu.cn

Authors

Jingpeng Wang − *State Key Laboratory of Oil and Gas Reservoir Geology and Exploitation, Southwest Petroleum University, Sichuan, Chengdu 610500, China; Xinjiang Oilfield Company of PetroChina, Karamay 834000, China*; orcid.org/0000-0002-2111-1688

Zongyu Lu − *Xinjiang Oilfield Company of PetroChina, Karamay 834000, China*

Wei Zhang − *Xinjiang Oilfield Company of PetroChina, Karamay 834000, China*

Jiwei Wu − *Xinjiang Oilfield Company of PetroChina, Karamay 834000, China*

Ruihua Wei − *Xinjiang Oilfield Company of PetroChina, Karamay 834000, China*

Xiaoxiao Li − *State Key Laboratory of Oil and Gas Reservoir Geology and Exploitation, Southwest Petroleum University, Sichuan, Chengdu 610500, China*

Complete contact information is available at: https://pubs.acs.org/10.1021/acsomega.2c00419

Notes

The authors declare no competing financial interest.

ACKNOWLEDGMENTS

The authors gratefully acknowledge the Major Technology Field Test Project of China National Petroleum Corporation (No. 2019F-33) for the financial support.

REFERENCES

(1) Nwaka, N.; Wei, C.; Chen, Y. "A Simplified Two-Phase Flow Model for Riser Gas Management With Non-Aqueous Drilling Fluids.". *ASME: J. Energy Resour. Technol.* **2020**, *142*, No. 103001. October

(2) Ibrahim, M. A.; Saleh, T. A. Synthesis of efficient stable dendrimer-modified carbon for cleaner drilling shale inhibition. *J. Environ. Chem. Eng.* **2020**, *9*, No. 104792.

(3) Saleh, T. A.; Ibrahim, M. A. Advances in functionalized Nanoparticles based drilling inhibitors for oil production. *Energy Rep.* **2019**, *5*, 1293−1304.

(4) Saleh, T. A.; Rana, A.; Arfaj, M. K. Graphene grafted with polyethyleneimine for enhanced shale inhibition in the water-based drilling fluid. *Environ. Nanotechnol., Monit. Manage.* **2020**, *14*, No. 100348.

(5) Hussain, M.; Amao, A. O.; Al-Ramadan, K.; Negara, A.; Saleh, T. A. (2020). Non-destructive techniques for linking methodology of geochemical and mechanical properties of rocksamples. *J. Pet. Sci. Eng.* **2020**, *195*, No. 107804.

(6) Al-Jamimi, H. A.; BinMakhashen, G. M.; Deb, K.; Saleh, T. A. Multiobjective optimization and analysis of petroleum refinery catalytic processes: A review. *Fuel* **2021**, *288*, No. 119678.

(7) Saleh, Tawfik A. Trends in the sample preparation and analysis of nanomaterials as environmental contaminants. *Trends Environ. Anal. Chem.* **2020**, *28*, No. e00101.

(8) Mahmoud, A. A.; Elkatatny, S.; Ahmed, S. A.; Mahmoud, M., 2018. Nanoclay Content Influence on Cement Strength for Oil Wells Subjected to Cyclic Steam Injection and High-Temperature Conditions. Paper SPE-193059-MS Presented at the 2018 Abu Dhabi International Petroleum Exhibition & Conference, Abu Dhabi, UAE,.*SPE*, 2018, 193059. DOI: 10.2118/193059-MS.

(9) Mahmoud, A. A.; Elkatatny, S. Mitigating CO_2 Reaction with Hydrated Oil Well Cement under Geologic Carbon Sequestration Using Nanoclay Particles. *J. Nat. Gas Sci. Eng.* **2019**, *68*, No. 102902.

(10) Ahmed, A.; Mahmoud, A. A.; Elkatatny, S.; Chen, W. The Effect of Weighting Materials on Oil-Well Cement Properties While Drilling Deep Wells. *Sustainability* **2019**, *11*, 6776.

(11) Pan, S.-Y.; Shah, K. J.; Chen, Y.-H.; Wang, M.-H.; Chiang, P.-C. Deployment of Accelerated Carbonation Using Alkaline Solid Wastes for Carbon Mineralization and Utilization Toward a Circular Economy. *ACS Sustainable Chem. Eng.* **2017**, 6429−6437.

(12) Haut, R. C.; Crook, R. J. Primary Cementing: Optimizing for Maximum Displacement. *World Oil* **1980**, 9−13.

(13) Haut, R. C.; Crook, R. J. (1982). *Laboratory Investigation ofLight Weight, Lo-Viscosity Cementing Spacer Fluids.* JPT.

(14) Zhang, Z.; Xiong, Y.; Guo, F. Analysis of wellbore temperature distribution and influencing factors during drilling horizontal wells. *J. Energy Resour. Technol.* **2018**, *140*, No. 092901.

(15) Tao, L. N.; Donovan, W. F. Through-flow in concentric and eccentric annuli of fine cleance with and without relative motion of the boundaries. *Trans. ASME* **1955**, *77*, 1291−1301.

(16) Heyda, J. F. A Green' s function solution for the case of non-concentric circular cylinders. *J. Franklin Inst.* **1959**, *267*, 25−34.

(17) Redberger, P. J.; Charles, M. E. Axial laminar flow in a circular pipe, containing a fixed eccentric core. *Can. J. Chem. Eng.* **1962**, *40*, 148−151.

(18) Vaughn, R. D. Axial Laminar Flow of Non-Newtonian Fluids in Narrow Eccentric Annuli. *Soc. Pet. Eng. J.* **1965**, *5*, 277−280.

(19) Iyoho, A. W.; Azar, J. J. An accurate slot_model for non_Newtonian fluid flow through eccentric annuli. *Soc. Pet. Eng. J.* **1981**, *21*, 565−572.

(20) Tosun, I. Axial laminar in an eccentric annulus:an approximate solution. *AIChE J.* **1984**, *30*, 877−878.

(21) Robertson, R. E.; Stiff, H. A. An improved rheological model for relating shear stress to shear rate in drilling fluids and cement slurries. *Trans. AIME* **1976**, *261*, 31.
(22) Beirute, R. M.; Flumerfelt, R. W. An evauction of the Robertson_Stiff model describing rheological properties of drilling fluids and cement slurries. *Soc. Pet. Eng. J.* **1986**, *17*, 97−100.
(23) Cloud, J. E.; Clark Stimulation, P. E. Stimulation fluid rheology:alternatives to the power_law fluid modelfor grosslinked gels. *SPE* **1980**, 11615.
(24) Li, M.; Ou, H.; Li, Z.; Gu, T.; Liu, H.; Guo, X. Contamination of cement slurries with diesel-based drilling fluids in a shale gas well. *J. Nat. Gas Sci. Eng.* **2015**, *27*, 1312−1320.
(25) Adamson, A. W.*Physical Chemistry of Surface*, 4th ed.; John wiley and Sons: New York, 1982; Vol. 25 02 pp 332−368.
(26) Salehi, R.; Paiaman, M. M. A novel cement slurry designapplicable to horizontal well conditions. *Pet. Coal* **2009**, *51*, 270−276.
(27) Pelipenko, S.; Frigaard, I. A. Mud removal and cement placement during primary cementing of an oil well. *J. Eng. Math.* **2004**, 1−16.
(28) Al Saedi, A. Q.; Flori, R. E.; Kabir, C. S. Estimating the initial-formation temperature and flowing-temperature gradient with transient-temperature analysis: Applications in gas reservoirs. *J. Nat. Gas Sci. Eng.* **2019**, *66*, 126−137.
(29) He, S.; Wang, W.; Tang, M.; Hu, B.; Xue, W. Effects of fluid seepage on wellbore stability of horizontal wells drilled underbalanced. *J. Nat. Gas Sci. Eng.* **2014**, *21*, 338−347.
(30) Reiber, L. E.; Archer, D. L.; Owens, W. W. A laboratory evaluation of the wettability of fifty oil reservoirs. *Soc. Pet. Eng. J.* **1972**, *4*, 531−540.
(31) Cuiec, L. E. Determination of the wettability of a sample of reservoir rock. *Reservoir Inst. France Pet.* **1978**, *33*, 705−728.
(32) Holbrook, O. C.; Bemard, G. G. Determination of wettability by dyeadsorption. *Trans. AME* **1958**, *213*, 261−264.
(33) Bashforth, F.; Adam, sJ. C.*An Attempt to Test the Theory of Capillary Action [M]*.Cambridge: Cambridge University Press,1892,*26*(03):34−38.
(34) Maze, C.; Burnet, G. A non-linear regression method for calculating surface tension and contact angle from the shape of a sessile drop. *Surf. Sci.* **1969**, *13*, 451−470.

https://doi.org/10.1021/acsomega.2c00419
ACS Omega 2022, 7, 37039−37049